

**Further results on  $O(a)$  improved lattice QCD  
to one-loop order of perturbation theory**

Stefan Sint

SCRI, The Florida State University,  
Tallahassee 32306-4052, Florida, U.S.A.

Peter Weisz

Max-Planck-Institut für Physik  
Föhringer Ring 6, D-80805 München, Germany

**Abstract**

We present results at one-loop order of perturbation theory for various improvement coefficients in on-shell  $O(a)$  improved lattice QCD. In particular we determine the additive counterterm required for on-shell improvement of the isovector vector current. Employing a general mass-independent renormalization scheme we also obtain the coefficients of the  $O(a)$  counterterms which are proportional to the quark mass in the improved isovector pseudo-scalar, axial vector and vector operators. In the latter case a comparison with a recent non-perturbative study is made.

April 1997

## 1. Introduction

This paper belongs to a series of publications on chiral symmetry and  $O(a)$  improvement in lattice QCD with Wilson quarks [1–6]. Here we report on the computation of various improvement coefficients to one-loop order of perturbation theory. The underlying theoretical framework is based on the Schrödinger functional (SF) [7,8] and has been presented in detail in the papers referred to above. In particular, a general overview can be obtained from refs. [1,2].

The present paper is organized as follows: In section 2 we recall various definitions limiting ourselves to those which are essential for the understanding of this paper. These include in particular the definitions of the on-shell  $O(a)$  improved isovector pseudo-scalar, axial vector and vector operators, and of the renormalized parameters and fields in a mass-independent renormalization scheme. We then summarize our main results which are contained in table 1 and eq. (2.16).

In section 3 we present a few details of the one-loop calculation and discuss the renormalization procedure for the general case of non-vanishing renormalized quark mass. Section 4 contains the determination of the improved vector current and of various improvement coefficients which arise in the case of non-zero quark mass. We end with a few concluding remarks (section 5). Finally, two appendices have been included which provide analytic expressions for the tree-level amplitudes and counterterms at zero and non-zero quark mass respectively.

## 2. Overview and results

A general introduction to on-shell  $O(a)$  improvement of lattice QCD with Wilson quarks can be found in ref. [3]. In particular there it has been discussed how the renormalization procedure can be carried out in a way consistent with  $O(a)$  improvement. In the following we adopt the conventions and notations as introduced in this reference.

## 2.1 Definitions

On-shell  $O(a)$  improvement requires the introduction of  $O(a)$  counterterms for both the lattice action and the composite fields of interest. The improved lattice action can be obtained by including the Sheikholeslami-Wohlert interaction term (with coefficient  $c_{\text{sw}}$ ) [9]. Concerning the composite fields we will restrict attention to a few gauge invariant combinations which are bilinear in the quark fields. Assuming  $N_f \geq 2$  mass degenerate quark flavours we consider the local isovector fields <sup>†</sup>,

$$V_\mu^a(x) = \bar{\psi}(x)\gamma_\mu\frac{1}{2}\tau^a\psi(x), \quad (2.1)$$

$$A_\mu^a(x) = \bar{\psi}(x)\gamma_\mu\gamma_5\frac{1}{2}\tau^a\psi(x), \quad (2.2)$$

$$P^a(x) = \bar{\psi}(x)\gamma_5\frac{1}{2}\tau^a\psi(x), \quad (2.3)$$

$$T_{\mu\nu}^a(x) = i\bar{\psi}(x)\sigma_{\mu\nu}\frac{1}{2}\tau^a\psi(x). \quad (2.4)$$

Using these definitions and following ref. [3] the improved isovector vector and axial vector currents may be parametrized as follows,

$$(V_{\text{I}})_\mu^a = V_\mu^a + c_V(g_0^2)a\frac{1}{2}(\partial_\nu^* + \partial_\nu)T_{\mu\nu}^a, \quad (2.5)$$

$$(A_{\text{I}})_\mu^a = A_\mu^a + c_A(g_0^2)a\frac{1}{2}(\partial_\mu^* + \partial_\mu)P^a. \quad (2.6)$$

Throughout the paper we will use a mass-independent renormalization scheme which is compatible with  $O(a)$  improvement. In such a scheme the renormalized coupling and quark mass are given by [3]

$$g_{\text{R}}^2 = \tilde{g}_0^2 Z_g(\tilde{g}_0^2, a\mu), \quad (2.7)$$

$$m_{\text{R}} = \tilde{m}_{\text{q}} Z_m(\tilde{g}_0^2, a\mu), \quad (2.8)$$

where  $\mu$  is the renormalization scale. The parameters  $\tilde{g}_0$  and  $\tilde{m}_{\text{q}}$  are defined as follows

$$\tilde{g}_0^2 = g_0^2 [1 + b_g(g_0^2)am_{\text{q}}], \quad (2.9)$$

$$\tilde{m}_{\text{q}} = m_{\text{q}} [1 + b_m(g_0^2)am_{\text{q}}], \quad m_{\text{q}} = m_0 - m_{\text{c}}, \quad (2.10)$$

---

<sup>†</sup> The Dirac gamma matrix conventions are as in appendix A of ref. [3]

where  $m_c$  is the critical bare quark mass.

With these definitions the renormalized improved currents and pseudo-scalar density take the form [3],

$$(V_R)_\mu^a = Z_V(\tilde{g}_0^2, a\mu) [1 + b_V(g_0^2)am_q] (V_I)_\mu^a, \quad (2.11)$$

$$(A_R)_\mu^a = Z_A(\tilde{g}_0^2, a\mu) [1 + b_A(g_0^2)am_q] (A_I)_\mu^a, \quad (2.12)$$

$$(P_R)^a = Z_P(\tilde{g}_0^2, a\mu) [1 + b_P(g_0^2)am_q] P^a. \quad (2.13)$$

In the massless theory on-shell correlation functions involving only these fields are  $O(a)$  improved if the improvement coefficients  $c_{sw}$ ,  $c_A$  and  $c_V$  are properly chosen as functions of the bare coupling  $g_0$ . In the presence of massive quarks one also needs to know the various  $b$ -coefficients introduced above.

To compute these coefficients we will consider correlation functions derived from the Schrödinger functional which involve the above operators and also the boundary quark fields  $\zeta, \bar{\zeta}$  and  $\zeta', \bar{\zeta}'$  [7].  $O(a)$  improved correlation functions are then obtained with the renormalized fields  $\zeta_R, \bar{\zeta}_R$  and  $\zeta'_R, \bar{\zeta}'_R$ , which are all related to the bare fields by the same renormalization factor, e.g.

$$\zeta_R = Z_\zeta(\tilde{g}_0^2, a\mu) [1 + b_\zeta(g_0^2)am_q] \zeta. \quad (2.14)$$

For completeness we recall that Schrödinger functional boundary conditions lead to additional cutoff effects which can be cancelled by counterterms that are localized at the boundaries. These boundary counterterms can be chosen such that the associated improvement coefficients  $c_{s,t}$  and  $\tilde{c}_{s,t}$  appear as weight factors for certain terms of the lattice action close to the boundaries [7,3].

## 2.2 Results

The computation of  $c_{sw}$  to one-loop order of perturbation theory was first performed in ref. [10] and the numerical result was confirmed to three significant digits in ref. [4]. For the purpose of our one-loop calculation it is sufficient to know that  $c_{sw} = 1$  at tree-level of perturbation theory.

The improvement coefficients  $c_A$  and  $c_V$  are given by

$$c_A = c_A^{(1)} g_0^2 + O(g_0^4), \quad c_A^{(1)} = -0.005680(2) \times C_F, \quad (2.15)$$

$$c_V = c_V^{(1)} g_0^2 + O(g_0^4), \quad c_V^{(1)} = -0.01225(1) \times C_F, \quad (2.16)$$

Table 1. Tree level and one-loop improvement coefficients  $b$

X	$b_X^{(0)}$	$b_X^{(1)}$
g	0	$0.012000(2) \times N_f$
m	$-\frac{1}{2}$	$-0.07217(2) \times C_F$
$\zeta$	$-\frac{1}{2}$	$-0.06738(4) \times C_F$
A	1	$0.11414(4) \times C_F$
V	1	$0.11492(4) \times C_F$
P	1	$0.11484(2) \times C_F$
T	1	

where  $C_F = (N^2 - 1)/2N$  for gauge group  $SU(N)$ . The coefficient  $c_A^{(1)}$  has first been obtained in ref. [4] and the computation of  $c_V^{(1)}$  will be presented in section 4. The extended numerical data produced in the course of this calculation also led to the improved estimate for  $c_A^{(1)}$  as given in eq. (2.15).

For the various  $b$ -coefficients, whose perturbation expansion reads

$$b = b^{(0)} + b^{(1)}g_0^2 + O(g_0^4), \quad (2.17)$$

we have collected the known results in table 1. The computation of  $b_g^{(1)}$  was performed in ref. [11] and the calculation of the remaining coefficients is the topic of section 4. It is remarkable that the coefficients  $b_A^{(1)}$ ,  $b_V^{(1)}$  and  $b_P^{(1)}$  are so close numerically. To our knowledge there is, however, no obvious theoretical explanation of this fact. Note also that all coefficients appear to be reasonably small, i.e. of  $O(1)$  when expanded in powers of  $g_0^2/4\pi$  for gauge group  $SU(3)$ .

In the case of  $b_V$  we can now make a comparison with the non-perturbative result for  $N_f = 0$  and gauge group  $SU(3)$  which was obtained in ref. [6]. An updated fit of the data, which reduces to the correct one-loop expression for small  $g_0$ , is given by <sup>†</sup>

$$b_V(g_0^2) = \frac{1 - 0.7613g_0^2 + 0.0012g_0^4 - 0.1136g_0^6}{1 - 0.9145g_0^2}, \quad 0 \leq g_0 \leq 1. \quad (2.18)$$

---

<sup>†</sup> We thank Hartmut Wittig for providing this fit and fig. 1.

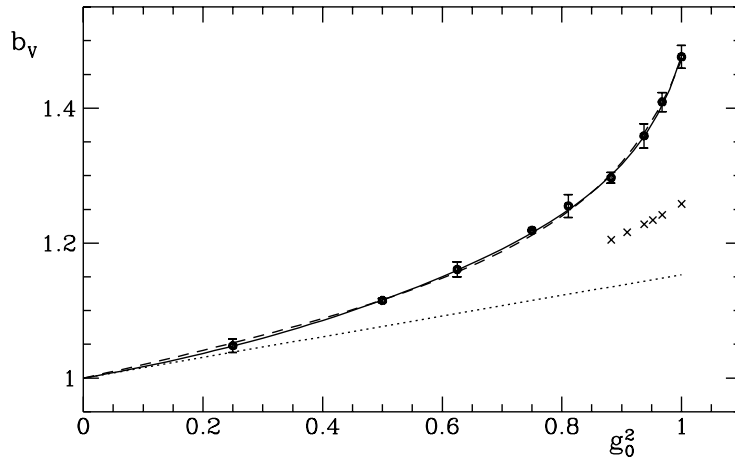


Fig. 1. The improvement coefficient  $b_V$  as a function of the bare coupling for gauge group SU(3). The data points and the fit function corresponding to the dashed curve are taken from ref. [6]. The solid curve is the new fit function (2.18), the dotted line is the perturbative result and the crosses denote the perturbative result when the coupling  $g_P$  is used instead of  $g_0$ .

The data together with the fit functions are displayed in fig. 1. Note that both curves are indistinguishable for all practical purposes.

Using the one-loop result for  $b_V$  we may also compare the data with so-called boosted perturbation theory. To this order this simply amounts to replacing the bare coupling  $g_0$  by Parisi's coupling  $g_P$  [12], defined by

$$g_P^2 = g_0^2/P, \quad (2.19)$$

where  $P$  denotes the expectation value of the plaquette in infinite volume. The corresponding values of  $b_V$  are plotted as crosses in fig. 1. Although the use of  $g_P$  moves the perturbative result towards the non-perturbative curve, there remains a significant discrepancy at the larger values of the bare coupling.

### 3. The one-loop calculation

We define the relevant correlation functions and provide some details of their evaluation to one-loop order of perturbation theory. This is followed by a discussion of the renormalization procedure for the general case of non-vanishing renormalized quark mass. In the following the reader is assumed to be familiar with ref. [4]. In particular the notation and the general set-up of perturbation theory on a finite lattice with Schrödinger functional boundary conditions will be taken over from this reference.

#### 3.1 Definition of the correlation functions

We consider the following correlation functions which were introduced in refs. [1,3],

$$f_A(x_0) = -a^6 \sum_{\mathbf{y}, \mathbf{z}} \frac{1}{3} \langle A_0^a(x) \bar{\zeta}(\mathbf{y}) \gamma_5 \frac{1}{2} \tau^a \zeta(\mathbf{z}) \rangle, \quad (3.1)$$

$$f_P(x_0) = -a^6 \sum_{\mathbf{y}, \mathbf{z}} \frac{1}{3} \langle P^a(x) \bar{\zeta}(\mathbf{y}) \gamma_5 \frac{1}{2} \tau^a \zeta(\mathbf{z}) \rangle. \quad (3.2)$$

Here and in the following we adopt the convention that repeated indices are summed over. To study the improved vector current (2.5) we also introduce the new correlation functions,

$$k_V(x_0) = -a^6 \sum_{\mathbf{y}, \mathbf{z}} \frac{1}{9} \langle V_k^a(x) \bar{\zeta}(\mathbf{y}) \gamma_k \frac{1}{2} \tau^a \zeta(\mathbf{z}) \rangle, \quad (3.3)$$

$$k_T(x_0) = -a^6 \sum_{\mathbf{y}, \mathbf{z}} \frac{1}{9} \langle T_{k0}^a(x) \bar{\zeta}(\mathbf{y}) \gamma_k \frac{1}{2} \tau^a \zeta(\mathbf{z}) \rangle. \quad (3.4)$$

The amplitudes above are sufficient for the determination of most of the improvement coefficients of sect. 2. However, in order to carry out a few additional checks we also calculated the boundary-to-boundary correlation  $f_1$ ,

$$f_1 = -\frac{a^{12}}{L^6} \sum_{\mathbf{u}, \mathbf{v}, \mathbf{y}, \mathbf{z}} \frac{1}{3} \langle \bar{\zeta}'(\mathbf{u}) \gamma_5 \frac{1}{2} \tau^a \zeta'(\mathbf{v}) \bar{\zeta}(\mathbf{y}) \gamma_5 \frac{1}{2} \tau^a \zeta(\mathbf{z}) \rangle, \quad (3.5)$$

which has previously appeared in the normalization conditions for the isovector axial vector and vector currents in refs. [1,6]. As an aside we recall that  $f_1$

will also be needed for the computation of the running quark mass in the SF scheme as defined in ref. [1]. A detailed discussion of this topic will be presented elsewhere [13,14].

### 3.2 Integration over the quark fields

The fermionic action being bilinear in the quark fields, the corresponding Grassmann integration can be carried out analytically using Wick's theorem. To write down the resulting expressions in a compact form we follow ref. [4] and introduce the matrix  $H(x)$  through

$$H(x) = a^3 \sum_{\mathbf{y}} \frac{\delta \psi_{\text{cl}}(x)}{\delta \rho(\mathbf{y})}. \quad (3.6)$$

Here  $\psi_{\text{cl}}$  denotes the classical solution of the Dirac equation in a given gauge field configuration and  $\rho$  is its boundary value at time  $x_0 = 0$ . One then finds

$$f_{\text{A}}(x_0) = -\frac{1}{2} \langle \text{tr} \{ H(x)^\dagger \gamma_0 H(x) \} \rangle_{\text{G}}, \quad (3.7)$$

$$f_{\text{P}}(x_0) = \frac{1}{2} \langle \text{tr} \{ H(x)^\dagger H(x) \} \rangle_{\text{G}}, \quad (3.8)$$

$$k_{\text{V}}(x_0) = -\frac{1}{6} \langle \text{tr} \{ \gamma_5 \gamma_k H(x)^\dagger \gamma_5 \gamma_k H(x) \} \rangle_{\text{G}}, \quad (3.9)$$

$$k_{\text{T}}(x_0) = \frac{1}{6} \langle \text{tr} \{ \gamma_5 \gamma_k H(x)^\dagger \gamma_5 \gamma_k \gamma_0 H(x) \} \rangle_{\text{G}}, \quad (3.10)$$

where the trace is over the Dirac and colour indices. The bracket  $\langle \dots \rangle_{\text{G}}$  means that expectation values have to be taken with the effective gauge field measure including the fermionic determinant.

In order to obtain a compact expression for  $f_1$  we follow ref. [6] and introduce the matrix

$$K = \tilde{c}_t \frac{a^3}{L^3} \sum_{\mathbf{x}} \left\{ P_+ U(x, 0)^{-1} H(x) \right\}_{x_0=T-a}. \quad (3.11)$$

Then one has

$$f_1 = \frac{1}{2} \langle \text{tr} \{ K^\dagger K \} \rangle_{\text{G}}. \quad (3.12)$$



### 3.3 Perturbation expansion

The perturbation expansion is now easily generated following ref. [4]. In particular we choose vanishing boundary gauge fields  $C$  and  $C'$  and take over the corresponding gauge fixing procedure. The gluon field is introduced in the standard way by parameterizing the link variables according to

$$U(x, \mu) = \exp\{ag_0q_\mu(x)\}. \quad (3.13)$$

As explained in ref. [4], the classical quark field and thus  $H(x)$  can be expanded in perturbation theory,

$$H(x) = H^{(0)}(x) + g_0H^{(1)}(x) + g_0^2H^{(2)}(x) + O(g_0^3). \quad (3.14)$$

Also expanding the boundary improvement coefficient [3],

$$\tilde{c}_t = 1 + \tilde{c}_t^{(1)}g_0^2 + O(g_0^4), \quad (3.15)$$

the corresponding expansion for  $K$  reads

$$K = K^{(0)} + g_0K^{(1)} + g_0^2K^{(2)} + O(g_0^3), \quad (3.16)$$

with

$$K^{(0)} = \frac{a^3}{L^3} \sum_{\mathbf{x}} P_+ H^{(0)}(T - a, \mathbf{x}), \quad (3.17)$$

$$K^{(1)} = \frac{a^3}{L^3} \sum_{\mathbf{x}} P_+ \left\{ H^{(1)}(x) - aq_0(x)H^{(0)}(x) \right\}_{x_0=T-a}, \quad (3.18)$$

$$K^{(2)} = \frac{a^3}{L^3} \sum_{\mathbf{x}} P_+ \left\{ H^{(2)}(x) - aq_0(x)H^{(1)}(x) + \frac{1}{2}[aq_0(x)]^2 H^{(0)}(x) + \tilde{c}_t^{(1)} H^{(0)}(x) \right\}_{x_0=T-a}. \quad (3.19)$$

Inserting these expansions in eqs. (3.7)–(3.10),(3.12) and carrying out the integrations over the gluon and ghost field variables finally leads to the desired expansion for the correlation functions,

$$f = f^{(0)} + g_0^2 f^{(1)} + O(g_0^4), \quad (3.20)$$

where  $f$  stands for any of the amplitudes in eqs. (3.1)–(3.5).

### 3.4 Tree level results

Explicit expressions for the tree level correlation functions  $f_A^{(0)}$  and  $f_P^{(0)}$  have been given in ref. [4]. The study of their approach to the continuum limit led to the determination of  $b_\zeta, b_m, b_A, b_P$  and  $c_A$  at lowest order of perturbation theory. To this order we have the relations

$$k_V^{(0)}(x_0) = \frac{2}{3}f_P^{(0)}(x_0) - \frac{1}{3}f_A^{(0)}(x_0), \quad (3.21)$$

$$k_T^{(0)}(x_0) = \frac{2}{3}f_A^{(0)}(x_0) - \frac{1}{3}f_P^{(0)}(x_0), \quad (3.22)$$

$$f_1^{(0)} = \left\{ \frac{1}{2}f_P^{(0)}(x_0) - \frac{1}{2}f_A^{(0)}(x_0) \right\}_{x_0=T-a}, \quad (3.23)$$

and we then find the tree level results  $b_V^{(0)} = b_T^{(0)} = 1$  and  $c_V^{(0)} = 0$ . All coefficients are thus known to lowest order of perturbation theory (cf. sect. 2).

### 3.5 Computation of $k_V^{(1)}$ and $f_1^{(1)}$

Except for the different Dirac structure the calculation of  $k_V^{(1)}$  is completely analogous to the cases of  $f_A^{(1)}$  and  $f_P^{(1)}$  treated in ref. [4]. In particular, there are again three diagrams to be computed which are the same as in fig. 1 of this reference (where the cross in this case denotes the vector vertex). The contribution of the quark boundary counterterm can also be inferred from there by noting

$$k_V^{(1)}(x_0)_b = \frac{2}{3}f_P^{(1)}(x_0)_b - \frac{1}{3}f_A^{(1)}(x_0)_b. \quad (3.24)$$

Note that the correlation function  $k_T^{(1)}$  could be computed along the same lines. However here,  $k_T$  is only encountered as an  $O(a)$  counterterm for the correlation function of the improved vector current (2.5). Since the associated improvement coefficient  $c_V$  vanishes at tree level we will only need the lowest order expression  $k_T^{(0)}$  in the following.

The correlation function  $f_1$  differs from the cases treated previously and therefore deserves a more detailed presentation. Inserting the expansion of the matrix  $K$  (3.16) in eq. (3.12) we obtain

$$\begin{aligned} f_1^{(1)} &= \frac{1}{2} \langle \text{tr} \{ K^{(1)\dagger} K^{(1)} \} \rangle_{\bar{G}} \\ &+ \frac{1}{2} \langle \text{tr} \{ K^{(2)\dagger} K^{(0)} + K^{(0)\dagger} K^{(2)} \} \rangle_{\bar{G}}. \end{aligned} \quad (3.25)$$

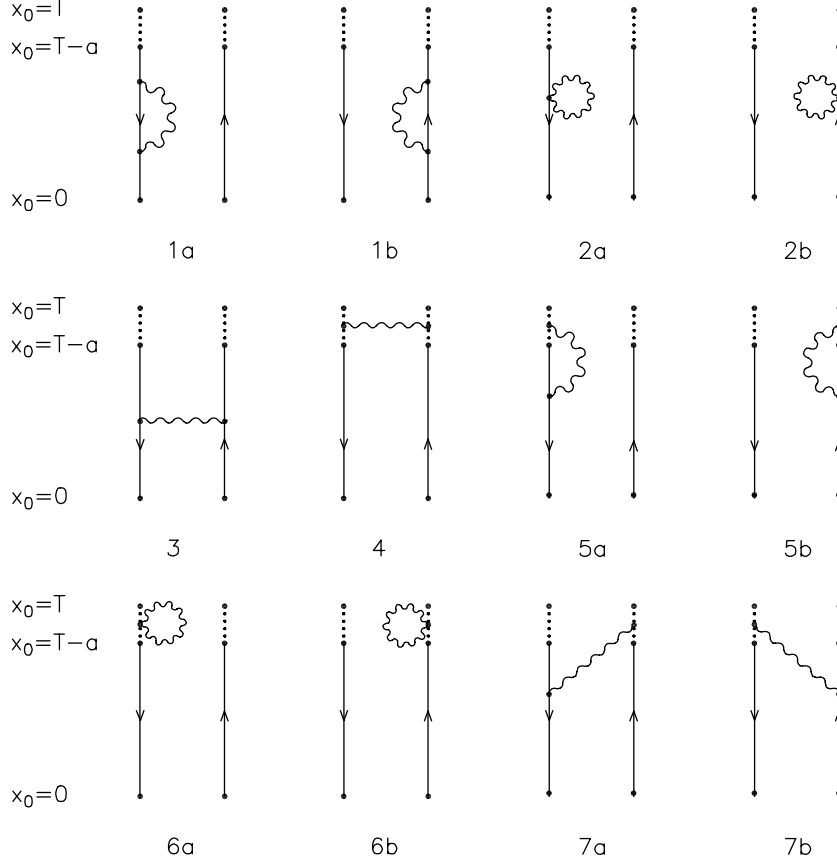


Fig. 2. Diagrams contributing to  $f_1$  at order  $g_0^2$ . The dotted lines symbolize the link from Euclidean time  $T - a$  to  $T$ .

Here, the bracket  $\langle \dots \rangle_{\tilde{G}}$  means the integration over the gluon and ghost fields as explained in ref. [4]. While the integration over the ghost fields is trivial at this order of perturbation theory, the integration over the gluon fields generates the diagrams displayed in fig. 2. The first three diagrams are similar to the ones computed for  $f_A, f_P$  and  $k_V$ , and the explicit link variables in eq. (3.11) lead to the additional diagrams 4 – 7.

Furthermore,  $f_1^{(1)}$  receives a contribution from the quark boundary counterterm which can be written in the form (see also eq. (4.31) of ref. [4])

$$f_{1b}^{(1)} = 2\tilde{c}_t^{(1)} f_1^{(0)} + \frac{1}{2} f_P^{(1)}(T - a)_b - \frac{1}{2} f_A^{(1)}(T - a)_b. \quad (3.26)$$

An explicit evaluation shows that this expression is indeed of order  $a$ , as expected.

On a lattice of a given size  $T/a \times (L/a)^3$  the Feynman diagrams can be evaluated numerically by inserting the explicit time-momentum representation of the propagators and vertices into the expressions for each diagram. For this purpose two independent Fortran programs were written and the final results were checked against each other and for gauge invariance. A fast version of one of the Fortran programs then enabled us to obtain numerical results for a relatively large range of lattice sizes, thus allowing for rather precise extrapolations to the continuum limit (cf. sect. 4).

### 3.6 Renormalized correlation functions

In order to take the limit of large  $L/a$  at fixed ratio  $T/L$  and physical length  $L$ , the bare parameters and fields have to be scaled such that the renormalized parameters and fields stay fixed. Furthermore this has to be done in a way consistent with  $O(a)$  improvement. It has been shown in ref. [3] that these requirements are met by any mass-independent renormalization scheme with the properties as summarized in sect. 2. In particular, the  $O(a)$  improvement coefficients introduced there are then independent of the renormalization conditions.

In perturbation theory a particularly convenient choice is the minimal subtraction scheme on the lattice which we shall adopt in the following. In this scheme all renormalization constants at a given order in the perturbation expansion in  $\tilde{g}_0^2$  are polynomials in  $\ln(a\mu)$  with mass-independent coefficients and no constant parts.

To first order of perturbation theory the substitutions for the coupling constant and the quark mass then amount to

$$g_0^2 = g_R^2 + O(g_R^4), \quad (3.27)$$

$$m_0 = m_0^{(0)} + g_R^2 m_0^{(1)} + O(g_R^4), \quad (3.28)$$

where the precise form of the coefficients,

$$m_0^{(0)} = \frac{1}{a} \left( 1 - \sqrt{1 - 2am_R} \right), \quad (3.29)$$

$$m_0^{(1)} = m_c^{(1)} - \frac{Z_m^{(1)} m_R - 2b_m^{(1)} (m_R - m_0^{(0)})}{\sqrt{1 - 2am_R}}, \quad (3.30)$$

is a direct consequence of the definitions made in sect. 2.

The renormalized correlation functions, defined by

$$[k_V(x_0)]_R = Z_V(1 + b_V am_q) Z_\zeta^2 (1 + b_\zeta am_q)^2 \times \{k_V(x_0) + ac_V \frac{1}{2} (\partial_0^* + \partial_0) k_T(x_0)\}, \quad (3.31)$$

$$[f_P(x_0)]_R = Z_P(1 + b_P am_q) Z_\zeta^2 (1 + b_\zeta am_q)^2 f_P(x_0), \quad (3.32)$$

$$[f_A(x_0)]_R = Z_A(1 + b_A am_q) Z_\zeta^2 (1 + b_\zeta am_q)^2 \times \{f_A(x_0) + ac_A \frac{1}{2} (\partial_0^* + \partial_0) f_P(x_0)\}, \quad (3.33)$$

$$[f_1]_R = Z_\zeta^4 (1 + b_\zeta am_q)^4 f_1, \quad (3.34)$$

have a well-defined perturbation expansion in the renormalized coupling  $g_R$ , with coefficients that are computable functions of  $a/L$ . However, to determine the  $O(a)$  improvement coefficients we only need to know the renormalized amplitudes up to terms of order  $a^2$ . Neglecting such terms, the expansion of  $[k_V]_R$  reads

$$[k_V(x_0)]_R = k_V^{(0)}(x_0) + g_R^2 \left\{ k_V^{(1)}(x_0) + m_0^{(1)} \frac{\partial}{\partial m_0} k_V^{(0)}(x_0) + \left( Z_V^{(1)} + 2Z_\zeta^{(1)} + am_R [b_V^{(1)} + 2b_\zeta^{(1)}] \right) k_V^{(0)}(x_0) + ac_V^{(1)} \frac{1}{2} (\partial_0^* + \partial_0) k_T^{(0)}(x_0) \right\} + O(g_R^4), \quad (3.35)$$

where it is understood that all quantities on the r.h.s. are evaluated at  $m_0 = m_0^{(0)}$  as given in eq. (3.29). Analogous expressions are obtained for  $[f_A]_R$  and  $[f_P]_R$ , in particular the case  $m_R = 0$  has already been discussed in ref. [4]. We thus directly proceed to the result for  $[f_1]_R$ ,

$$[f_1]_R = (1 - 2am_R) \left[ f_1^{(0)} + g_R^2 \left\{ f_1^{(1)} + m_0^{(1)} \frac{\partial}{\partial m_0} f_1^{(0)} + \left( 4Z_\zeta^{(1)} + am_R [4b_\zeta^{(1)} + 2Z_m^{(1)}] \right) f_1^{(0)} \right\} \right] + O(g_R^4). \quad (3.36)$$

Since we are neglecting terms of order  $a^2$ , the expansion

$$m_0^{(1)} = m_c^{(1)} - m_R \left[ Z_m^{(1)} + a m_R \left( Z_m^{(1)} + b_m^{(1)} \right) \right] + \mathcal{O}(a^2), \quad (3.37)$$

may be inserted in eqs. (3.35),(3.36). However, note that we do not directly expand the coefficient  $m_0^{(0)}$  [eq. (3.29)]. One has to be careful here because the bare one-loop amplitudes are linearly divergent. While the additive renormalization of the quark mass removes these divergences, the correct evaluation of the renormalized amplitudes to  $\mathcal{O}(a)$  requires a consistent treatment of  $m_0^{(0)}$  to order  $a^2$ , in both the bare one-loop amplitudes and the mass counterterms. It thus appears safer to first carry out the renormalization procedure using the exact coefficient and only neglect terms of  $\mathcal{O}(a^2)$  in the final result for the renormalized correlation functions.

#### 4. Computation of the improvement coefficients

The improvement coefficients can be determined by requiring an improved continuum limit behaviour of the renormalized correlation functions. We first consider the case of vanishing renormalized quark mass and compute  $c_V^{(1)}$ . We then turn to the massive case and also determine the  $b$ -coefficients.

##### 4.1 Choice of parameters

For the numerical analysis of the renormalized amplitudes one needs to make a choice for the kinematical parameters  $T, L, x_0, \theta$  and the quark mass  $m_R$ . Following ref. [4] we choose  $T = 2L$  and  $x_0 = T/2$ . Setting  $z = m_R L$  we define the dimensionless functions,

$$h_P(\theta, z, a/L) = [f_P(x_0)]_R \Big|_{x_0=T/2}, \quad (4.1)$$

$$h_A(\theta, z, a/L) = [f_A(x_0)]_R \Big|_{x_0=T/2}, \quad (4.2)$$

$$h_V(\theta, z, a/L) = [k_V(x_0)]_R \Big|_{x_0=T/2}, \quad (4.3)$$

$$h_{dA}(\theta, z, a/L) = L \frac{1}{2} (\partial_0^* + \partial_0) [f_A(x_0)]_R \Big|_{x_0=T/2}, \quad (4.4)$$

$$h_1(\theta, z, a/L) = [f_1]_R. \quad (4.5)$$

From the discussion in sect. 3 one then infers the form of  $h_P$ ,  $h_{dA}$  and  $h_1$

$$h_P = u_0 + g_R^2 \left\{ u_1 + \tilde{c}_t^{(1)} u_2 + am_0^{(1)} u_3 + \left( Z_P^{(1)} + 2Z_\zeta^{(1)} + \frac{a}{L} z [b_P^{(1)} + 2b_\zeta^{(1)}] \right) u_0 \right\} + O(g_R^4), \quad (4.6)$$

$$h_{dA} = w_0 + g_R^2 \left\{ w_1 + \tilde{c}_t^{(1)} w_2 + am_0^{(1)} w_3 + c_A^{(1)} w_4 + \left( Z_A^{(1)} + 2Z_\zeta^{(1)} + \frac{a}{L} z [b_A^{(1)} + 2b_\zeta^{(1)}] \right) w_0 \right\} + O(g_R^4), \quad (4.7)$$

$$h_1 = t_0 + g_R^2 \left\{ t_1 + \tilde{c}_t^{(1)} t_2 + am_0^{(1)} t_3 + \left( 4Z_\zeta^{(1)} + \frac{a}{L} z [4b_\zeta^{(1)} + 2Z_m^{(1)}] \right) t_0 \right\} + O(g_R^4). \quad (4.8)$$

Similarly we find,

$$h_A = v_0 + g_R^2 \left\{ v_1 + \tilde{c}_t^{(1)} v_2 + am_0^{(1)} v_3 + c_A^{(1)} v_4 + \left( Z_A^{(1)} + 2Z_\zeta^{(1)} + \frac{a}{L} z [b_A^{(1)} + 2b_\zeta^{(1)}] \right) v_0 \right\} + O(g_R^4), \quad (4.9)$$

and the same for  $h_V$ , with the subscript A replaced by V and the coefficients  $v_i$  replaced by  $y_i$ .

All the coefficients are still functions of  $\theta$  and  $z$ . Analytic expressions can be derived for those coefficients which derive from the tree level correlation functions or the  $O(a)$  counterterms. Their expansions to order  $a/L$  for the special case of  $z = 0$  and non-vanishing  $\theta$  are given in appendix A and in appendix B of ref. [4]. In appendix B we give the corresponding results for  $\theta = 0$  and non-vanishing renormalized quark mass.

The coefficients  $v_1, y_1, u_1, w_1$  and  $t_1$  are only obtained numerically so that we must choose specific values for the parameters  $\theta$  and  $z$ . In the case of vanishing quark mass  $z = 0$  we decided to collect numerical data for the three

values  $\theta = 0$ ,  $\theta = 0.1$  and  $\theta = 1$ . In the massive case we set  $\theta = 0$  and chose the three values  $z = 0.1$ ,  $z = 0.5$  and  $z = 1$ .

With the above choices for the parameters the Feynman diagrams were then evaluated numerically in 128 bit precision arithmetic for a sequence of lattice sizes ranging from  $L/a = 4$  to  $L/a = 48$ .

#### 4.2 Logarithmic divergences

In the minimal subtraction scheme the one-loop renormalization constants all take the form

$$Z(\tilde{g}_0^2, a\mu) = 1 + Z^{(1)}\tilde{g}_0^2 + \mathcal{O}(\tilde{g}_0^4), \quad (4.10)$$

where  $Z^{(1)}$  is proportional to  $\ln(a\mu)$ . From analytical results obtained with conventional perturbative techniques one then expects [15–17,8]

$$Z_A^{(1)} = Z_V^{(1)} = 0, \quad (4.11)$$

and

$$Z_P^{(1)} = -Z_m^{(1)} = -2Z_\zeta^{(1)} = \frac{6C_F}{(4\pi)^2} \ln(a\mu). \quad (4.12)$$

In the course of our computation we were able to determine the coefficients of the logarithmic divergences numerically to high precision. The results were in complete agreement with the above expectations and will not be further discussed. In the numerical analysis presented below we set  $\mu = 1/L$  and use the exact coefficients when subtracting the logarithmically divergent parts.

#### 4.3 Computation of $c_V^{(1)}$

For vanishing quark mass the analogue of eq. (4.9) for  $h_V$  simplifies to

$$\begin{aligned} h_V(\theta, 0, a/L) = & y_0 + g_R^2 \left[ y_1 + \tilde{c}_t^{(1)} y_2 + am_c^{(1)} y_3 \right. \\ & \left. + \left( Z_V^{(1)} + 2Z_\zeta^{(1)} \right) y_0 + c_V^{(1)} y_4 \right] + \mathcal{O}(g_R^4). \end{aligned} \quad (4.13)$$

In order to extract  $c_V^{(1)}$  one can for example demand  $\mathcal{O}(a)$  improvement of the combination  $h_V - \frac{1}{3}(2h_P - h_A)$ . Due to the identities (3.21) and (3.24) the coefficients  $\tilde{c}_t^{(1)}$  and  $am_c^{(1)}$  do not contribute and the improvement condition then reads

$$y_1 - \frac{1}{3}(2u_1 - v_1) - \frac{2}{3}Z_P^{(1)} u_0 - \frac{1}{3}(c_V^{(1)} - c_A^{(1)})v_4 = \text{const} + \mathcal{O}(a^2). \quad (4.14)$$



Here we have anticipated the absence of  $O(a)$  effects proportional to  $\ln(L/a)$ , which are cancelled by setting the coefficient of the Sheikholeslami-Wohlert term to  $c_{\text{sw}} = 1$ . We have checked in a number of cases that this indeed happens. Defining

$$\mathcal{C}(L) = y_1 - \frac{1}{3}(2u_1 - v_1) + \frac{C_{\text{F}}}{4\pi^2}u_0 \ln(L/a), \quad (4.15)$$

and the symmetric difference operator

$$\frac{1}{2}(\partial + \partial^*)\mathcal{C}(L) = \frac{1}{2a} \left[ \mathcal{C}(L+a) - \mathcal{C}(L-a) \right], \quad (4.16)$$

we find

$$c_{\text{V}}^{(1)} - c_{\text{A}}^{(1)} = - \lim_{L/a \rightarrow \infty} \frac{3L}{v_4} \frac{1}{2}(\partial + \partial^*)\mathcal{C}(L). \quad (4.17)$$

It turns out that the  $O(a/L)$  corrections in the expression above are large for both values of  $\theta$  considered and the extrapolation must therefore be done carefully. We used the method described in ref. [18], appropriately adapted to the present case and finally obtained

$$c_{\text{V}}^{(1)} - c_{\text{A}}^{(1)} = -0.00657(1) \times C_{\text{F}}. \quad (4.18)$$

Insertion of the numerical value for  $c_{\text{A}}^{(1)}$  [eq. (2.15)] then leads to the result quoted in eq. (2.16).

An alternative determination of  $c_{\text{V}}^{(1)}$  can be obtained by requiring  $O(a)$  improvement of the ratio  $h_{\text{V}}(\theta, 0, a/L)/h_{\text{V}}(0, 0, a/L)$ . With the results of appendix A this is equivalent to demanding

$$y_1 - \frac{1}{N}y_0(y_1)_{\theta=0} + am_{\text{c}}^{(1)} \left( y_3 + 2y_0 \frac{L}{a} \right) + c_{\text{V}}^{(1)}y_4 + \tilde{c}_{\text{t}}^{(1)}y_2 = \text{const} + O(a^2). \quad (4.19)$$

While the renormalization constants cancel in this ratio we now need to know the one-loop coefficient  $m_{\text{c}}^{(1)}$  of the critical bare quark mass. We here follow ref. [4] and use the relation

$$(w_1/w_3)_{\theta=z=0} = -am_{\text{c}}^{(1)} + O(a^3/L^3). \quad (4.20)$$

We then define the combination

$$\mathcal{C}'(L) = y_1 - \frac{1}{N}y_0(y_1)_{\theta=0} - \left( y_3 + 2y_0 \frac{L}{a} \right) (w_1/w_3)_{\theta=z=0}, \quad (4.21)$$

where it is understood that  $w_1$  and  $w_3$  are computed at the same lattice size as the other coefficients. With the results of appendix A we then find

$$c_V^{(1)} + 4 \frac{\cosh(2\sqrt{3}\theta) + 1}{\cosh(2\sqrt{3}\theta)} \tilde{c}_t^{(1)} = \lim_{L/a \rightarrow \infty} \frac{L}{y_4} \frac{1}{2} (\partial + \partial^*) \mathcal{C}'(L). \quad (4.22)$$

Evaluation of this relation at two different values of  $\theta$  allows to eliminate  $\tilde{c}_t^{(1)}$  and thus leads to a direct determination of  $c_V^{(1)}$ . Complete consistency with the previous method was found.

With our extended data we now also obtain a slightly more accurate estimate of  $\tilde{c}_t^{(1)}$  than the one given in ref. [4], viz.

$$\tilde{c}_t^{(1)} = -0.01346(1) \times C_F. \quad (4.23)$$

#### 4.4 Computation of the $b$ -coefficients to one-loop order

In order to compute the  $b$ -coefficients to one-loop order we now consider the massive case where  $z = m_R L$  is kept fixed at a non-zero value. In the following we always assume  $\theta = 0$  and use the coefficients given in appendix B.

We start by considering  $h_1$  [eq. (4.8)], which can be written in the form

$$h_1 = N e^{-4z} \left[ 1 + g_R^2 \left\{ \mathcal{T}(L) + 4z (b_\zeta^{(1)} + \tilde{c}_t^{(1)} + z b_m^{(1)}) \frac{a}{L} \right\} + \mathcal{O}(g_R^4) \right]. \quad (4.24)$$

Using the exact results for the logarithmic divergences we have defined

$$\mathcal{T}(L) = N^{-1} e^{4z} \left[ t_1 + a m_c^{(1)} t_3 \right] + 2(1 + 2z) \frac{6C_F}{(4\pi)^2} \ln(L/a). \quad (4.25)$$

To evaluate  $\mathcal{T}(L)$  numerically on a lattice of size  $L/a$ , we here again follow the procedure above and replace the coefficient  $a m_c^{(1)}$  by the ratio  $-(w_1/w_3)_{\theta=z=0}$ , computed for the same lattice size. Requiring improvement of  $h_1$  then determines the linear combination of improvement coefficients,

$$4z \left[ \tilde{c}_t^{(1)} + b_\zeta^{(1)} + z b_m^{(1)} \right] = \lim_{L/a \rightarrow \infty} (L^2/a) \frac{1}{2} (\partial + \partial^*) \mathcal{T}(L). \quad (4.26)$$

Since  $\tilde{c}_t^{(1)}$  is already known,  $b_\zeta^{(1)}$  and  $b_m^{(1)}$  can be determined by evaluating the improvement condition at two different values of the quark mass.

We can proceed similarly for the other correlation functions  $f_P, f_A$  and  $k_V$ . We here require the improved continuum limit behaviour for the ratios  $h_P^2/h_1, h_A^2/h_1$ , and  $h_V^2/h_1$ . Defining

$$\mathcal{U}(L) = N^{-1}e^{2z} \left[ u_1 + am_c^{(1)} u_3 \right] + 2z \frac{6C_F}{(4\pi)^2} \ln(L/a), \quad (4.27)$$

$$\mathcal{V}(L) = -N^{-1}e^{2z} \left[ v_1 + am_c^{(1)} v_3 \right] + (1 + 2z) \frac{6C_F}{(4\pi)^2} \ln(L/a), \quad (4.28)$$

$$\mathcal{Y}(L) = N^{-1}e^{2z} \left[ y_1 + am_c^{(1)} y_3 \right] + (1 + 2z) \frac{6C_F}{(4\pi)^2} \ln(L/a), \quad (4.29)$$

we find e.g.

$$\frac{1}{N} \frac{h_V^2}{h_1} = 1 + g_R^2 \left[ 2\mathcal{Y}(L) - \mathcal{T}(L) + 2z \frac{a}{L} (2c_V^{(1)} + b_V^{(1)}) \right] + \mathcal{O}(g_R^4). \quad (4.30)$$

Similar expressions can be derived for the other cases and we thus find that  $\mathcal{O}(a)$  improvement requires

$$zb_P^{(1)} = \lim_{L/a \rightarrow \infty} (L^2/a) \frac{1}{2} (\partial + \partial^*) \left[ \mathcal{U}(L) - \frac{1}{2} \mathcal{T}(L) \right], \quad (4.31)$$

$$z \left[ 2c_A^{(1)} + b_A^{(1)} \right] = \lim_{L/a \rightarrow \infty} (L^2/a) \frac{1}{2} (\partial + \partial^*) \left[ \mathcal{V}(L) - \frac{1}{2} \mathcal{T}(L) \right], \quad (4.32)$$

$$z \left[ 2c_V^{(1)} + b_V^{(1)} \right] = \lim_{L/a \rightarrow \infty} (L^2/a) \frac{1}{2} (\partial + \partial^*) \left[ \mathcal{Y}(L) - \frac{1}{2} \mathcal{T}(L) \right]. \quad (4.33)$$

The evaluation of the various improvement conditions was done using the methods of ref. [18] and led to the numerical results as quoted in table 1. Various consistency checks were made by studying different combinations of correlation functions. For example, a more direct determination of  $b_m^{(1)}$  was obtained by considering the ratio  $h_{dA}(0, z, a/L)/h_A(0, z, a/L)$ . As a further confirmation of the conceptual framework, we have also analyzed data at finite renormalized quark mass and values of  $\theta \neq 0$  and verified that the  $b$ -coefficients are indeed independent of  $\theta$ .

## 5. Concluding remarks

This paper presents a further step in a systematic investigation of the continuum limit of lattice QCD. At one-loop order of perturbation theory we have studied the continuum limit of many different renormalized amplitudes. Various non-trivial consistency checks have been carried out, for both zero and non-zero renormalized quark mass. As a result our analysis further supports the consistency of the general framework of on-shell  $O(a)$  improvement as presented in ref. [3].

The  $O(a)$  improvement coefficients which enter the definition of the improved lattice action and the quark bilinear isovector pseudo-scalar, vector and axial vector operators are now all known to one-loop order of perturbation theory. The ultimate aim is of course to compute the same coefficients non-perturbatively. This has been partially achieved for the quenched theory (i.e. for  $N_f = 0$ ) in refs. [5,6]. More precisely, the coefficients  $c_{sw}, c_A$  and  $b_V$  have been determined for this case and a similar determination of  $c_V$  is under way [19]. The extension to the full theory with two quark flavours has also been initiated and first results are expected in the near future [20].

However, the non-perturbative methods developed so far cannot be used in a straightforward manner to determine all of the improvement coefficients. An example is the coefficient  $b_A$  for which one presently has to rely on perturbative estimates. Of course, this does not represent a severe limitation provided the quark mass (measured in lattice units) is small enough. In this context it may be of some interest that the perturbative results for  $b_V$  and  $b_A$  are approximately of the same magnitude. While this need not remain true at higher orders or beyond perturbation theory it is certainly tempting to use the non-perturbative result for  $b_V$  as a first guess for  $b_A$ .

### *Acknowledgements*

This work is part of the ALPHA collaboration research programme. We would like to thank our colleagues Martin Lüscher, Rainer Sommer and Hartmut Wittig for helpful discussions and critical comments on a first draft of this paper. Stefan Sint thanks the Max-Planck-Institut for hospitality and acknowledges support by the U.S. Department of Energy (contracts DE-FG05-85ER250000 and DE-FG05-96ER40979).

## Appendix A

For the massless case  $z = m_{\text{R}}L = 0$ , the expansions of the functions  $u_i, v_i$  and  $w_i$  (for  $i \neq 1$ ) have been given in appendix B of ref. [4], up to corrections of order  $(a/L)^2$ . Our definitions then imply

$$y_i = \frac{2}{3}u_i - \frac{1}{3}v_i \quad \text{for } i = 0, 2, 3, \quad (\text{A.1})$$

$$y_4 = -\frac{1}{3}v_4 + \frac{2}{3}w_0 \frac{a}{L}. \quad (\text{A.2})$$

Using the abbreviations

$$\text{co} = \cosh(2\sqrt{3}\theta), \quad \text{si} = \sinh(2\sqrt{3}\theta), \quad (\text{A.3})$$

we also give the explicit expressions,

$$y_0 = \frac{N(2\text{co} + 1)}{3\text{co}^2}, \quad (\text{A.4})$$

$$y_2 = \frac{8N\theta \text{si}(\text{co} + 1)}{\sqrt{3}\text{co}^3} \frac{a}{L}, \quad (\text{A.5})$$

$$y_3 = -\frac{N \text{si}(\text{co} + 2)}{3\sqrt{3}\theta \text{co}^3} \frac{L}{a} - \left\{ \frac{N\theta \text{si}(\text{co} + 2)}{18\sqrt{3}\text{co}^3} + \frac{4N\theta^2}{9\text{co}^4} (\text{co}^3 + 4\text{co}^2 - 2\text{co} - 6) \right\} \frac{a}{L}, \quad (\text{A.6})$$

$$y_4 = \frac{2N\theta \text{si} a}{\sqrt{3}\text{co}^2 L}. \quad (\text{A.7})$$

For the functions  $t_i$  introduced in eq. (4.8) we obtain

$$t_0 = \frac{N}{\text{co}^2}, \quad (\text{A.8})$$

$$t_2 = \frac{24N\theta \text{si} a}{\sqrt{3}\text{co}^3 L}, \quad (\text{A.9})$$

$$t_3 = -\frac{2N \text{si} L}{\sqrt{3}\theta \text{co}^3 a} + \frac{2N}{\text{co}^2}$$

$$- \left\{ \frac{19N\theta \text{si}}{3\sqrt{3}\text{co}^3} - \frac{8N\theta^2(1-2\text{si}^2)}{3\text{co}^4} \right\} \frac{a}{L}. \quad (\text{A.10})$$

## Appendix B

In this appendix we provide explicit expressions for the coefficient functions introduced in eqs. (4.6)–(4.9), for the special case  $\theta = 0$ . We set  $z = m_{\text{R}}L$  and use the tree level expression of the renormalized quark mass,  $m_{\text{R}} = m_0(1 - am_0/2)$ . Up to terms of order  $a^2/L^2$  we then find

$$t_0 = Ne^{-4z}, \quad (\text{B.1})$$

$$t_2 = Ne^{-4z} 4z \frac{a}{L}, \quad (\text{B.2})$$

$$t_3 = Ne^{-4z} \left\{ -4\frac{L}{a} + 2 + 4z + 2z\left(\frac{8}{3}z^2 + 3z - 1\right) \frac{a}{L} \right\}, \quad (\text{B.3})$$

$$u_0 = Ne^{-2z}, \quad (\text{B.4})$$

$$u_2 = Ne^{-2z} 2z \frac{a}{L}, \quad (\text{B.5})$$

$$u_3 = Ne^{-2z} \left\{ -2\frac{L}{a} + 2z + z^2\left(\frac{4}{3}z - 1\right) \frac{a}{L} \right\}, \quad (\text{B.6})$$

$$v_i = -u_i \quad \text{for } i = 0, 2, 3, \quad (\text{B.7})$$

$$v_4 = -Ne^{-2z} 2z \frac{a}{L}, \quad (\text{B.8})$$

$$w_0 = Ne^{-2z} 2z, \quad (\text{B.9})$$

$$w_2 = Ne^{-2z} 4z^2 \frac{a}{L}, \quad (\text{B.10})$$

$$w_3 = Ne^{-2z} \left\{ (2 - 4z) \frac{L}{a} + 4z^2 - 2z \right\}$$

$$+ z^2 \left( 5 - \frac{22}{3} z + \frac{8}{3} z^2 \right) \frac{a}{L} \}, \quad (\text{B.11})$$

$$w_4 = N e^{-2z} 4z^2 \frac{a}{L}, \quad (\text{B.12})$$

$$y_i = -v_i \quad \text{for} \quad i = 0, 2, 3, 4. \quad (\text{B.13})$$

### References

- [1] K. Jansen, C. Liu, M. Lüscher, H. Simma, S. Sint, R. Sommer, P. Weisz and U. Wolff, Phys. Letts. B372 (1996) 275
- [2] M. Lüscher, S. Sint, R. Sommer, P. Weisz, H. Wittig and U. Wolff, Nucl. Phys. B (Proc. Suppl.) 53 (1997) 905
- [3] M. Lüscher, S. Sint, R. Sommer and P. Weisz, Nucl. Phys. B478 (1996) 365
- [4] M. Lüscher and P. Weisz, Nucl. Phys. B479 (1996) 429
- [5] M. Lüscher, S. Sint, R. Sommer, P. Weisz and U. Wolff, Non-perturbative  $O(a)$  improvement of lattice QCD, hep-lat/9609035, accepted for publication in Nucl. Phys. B
- [6] M. Lüscher, S. Sint, R. Sommer and H. Wittig, Non-perturbative determination of the axial current normalization constant in  $O(a)$  improved lattice QCD, hep-lat/9611015, accepted for publication in Nucl. Phys. B
- [7] M. Lüscher, R. Narayanan, P. Weisz and U. Wolff, Nucl. Phys. B384 (1992) 168
- [8] S. Sint, Nucl. Phys. B421 (1994) 135, Nucl. Phys. B451 (1995) 416
- [9] B. Sheikholeslami and R. Wohlert, Nucl. Phys. B259 (1985) 572
- [10] R. Wohlert, Improved continuum limit lattice action for quarks, DESY preprint 87-069 (1987), unpublished
- [11] S. Sint and R. Sommer, Nucl. Phys. B465 (1996) 71
- [12] G. Parisi, in: High-Energy Physics — 1980, XX. Int. Conf. Madison (1980), ed. L. Durand and L. G. Pondrom (American Institute of Physics, New York, 1981)
- [13] S. Sint and P. Weisz, work in progress
- [14] M. Lüscher, R. Sommer and H. Wittig, work in progress

- [15] E. Gabrielli, G. Martinelli, C. Pittori, G. Heatlie and C. T. Sachrajda, Nucl. Phys. B362 (1991) 475
- [16] M. Göckeler et al., Nucl. Phys. B (Proc. Suppl.) 53 (1997) 896
- [17] S. Sint, private notes (1993,1996)
- [18] M. Lüscher and P. Weisz, Nucl. Phys. B266 (1986) 309
- [19] M. Guagnelli and R. Sommer, work in progress
- [20] K. Jansen and R. Sommer, work in progress